GEOPHYSICAL RESEARCH LETTERS, VOL. 26, NO. 9, PAGES 1235-1238, MAY 1, 1999

Two-Dimensional Structure of the Co-Planar and Non-Coplanar Magnetopause During Reconnection

D. Krauss-Varban[1], H. Karimabadi[1] and N. Omidi[1,2]
SciberNet, Inc., San Diego, CA

Abstract. The two-dimensional (2-D) magnetopause transition during reconnection is investigated with large-scale hybrid simulations. Contrary to previous studies, but in agreement with observations, the two discontinuities that form are not an intermediate shock or a slow shock. A 2-D reconnection configuration develops with jumps that do not satisfy Rankine-Hugoniot conditions of known discontinuities. All plasma quantities are fairly constant between the discontinuities. This region is characterized by a nearly unchanged sheath density, slight temperature enhancement, and significant magnetic field depression and thus resembles the "Sheath Transition Layer" of *Song et al.* [1989]. For a non-coplanar magnetic field $B_{z\circ}$, the plasma β attains very high values on the outflow side where $B_{z\circ}$ and the Hall-generated field cancel, and the jet becomes unstable. In this case, the magnetosheath-side discontinuity resembles the often-observed rotational discontinuity.

1. Introduction

Configurations describing quasi steady-state reconnection were introduced by *Petschek* [1964] for the symmetric case (identical parameters on both sides) and by *Levy et al.* [1964] for asymmetric magnetopause reconnection, as for southward interplanetary magnetic field (IMF). More general magnetohydrodynamic (MHD) calculations have been performed since [*Sonnerup,* 1979; *Scholer,* 1989; *Lin and Lee,* 1993]. It is usually assumed that a succession of 1-D discontinuities accomplishes the required transition. In the asymmetric case, solution of the MHD Riemann problem [*Lin and Lee,* 1993] predicts a rotational discontinuity (RD), a contact discontinuity (CD), and a slow shock (SS) when crossing from the magnetosheath ($\mathbf{B}_\circ$) to the magnetosphere ($\mathbf{B}_1$). A slow expansion wave is situated between the RD and the CD. Resistive MHD [*Scholer,* 1989; *Lin and Lee,* 1993] suggest that in the coplanar case ($\mathbf{B}_\circ$ and $\mathbf{B}_1$ in one plane), an intermediate shock (IS) takes on the role of the RD, while there is a time-dependent IS (TDIS) in the non-coplanar case (finite guide field).

Much evidence exists for both patchy, time-dependent [*Russell and Elphic,* 1978] and quasi steady-state reconnection at the magnetopause [*Gosling at al.,* 1990, and references]. Nevertheless, to date there are no observations of the above succession of discontinuities, and no strong evidence of SSs on the magnetospheric side.

It is suspected that ion-kinetic processes are responsible for the above discrepancies. In fact, 1-D hybrid simulations demonstrate that a CD cannot form because of ion transport [*Omidi and Winske,* 1995]. The first large-scale hybrid simulations [*Krauss-Varban and Omidi,* 1995; *Lin and Swift,* 1996; *Kuznetsova et al.,* 1996; also *Lottermoser et al.,* 1998] address tail reconnection, and as such deal with the low β lobe and symmetric case, resulting in discontinuities different from what is expected or observed at the magnetopause. In recent 2-D hybrid simulations of the coplanar magnetopause, *Lin and Xie* [1997] found an IS on the sheath side and a second discontinuity on the magnetospheric side, which both do not conform to typical observations. However, this may be due to the fact that the coplanar situation is a singular case. Thus, it remains open whether kinetic effects are the sole reason for the failure of simulations to describe the observations.

While RDs are often observed [*Berchem and Russell,* 1982], many magnetopause crossings under southward IMF conditions suggest a different picture. For example, *Song et al.* [1989] observed a "sheath transition layer" bounded by two discontinuities of approximately switch-off character. However, the density is almost unchanged from the sheath, making it impossible to interpret the first discontinuity as an IS. Furthermore, the temperature is only slightly enhanced from the sheath, and much smaller than in the magnetosphere. No MHD discontinuity with finite B-normal and jump in B allows for a temperature decrease from the magnetosphere into the layer. Thus, in general it may not be possible to interpret magnetopause observations in the framework of 1-D discontinuities. We are left with a situation where neither the above type of discontinuities nor RDs are seen in kinetic magnetopause reconnection simulations.

Motivated by the discrepancy between the observations and published simulations, we have conducted a number of simulations taking special care that the boundary conditions do not influence the solution. We find two simple discontinuities that share many features with the observations by *Song et al.* [1989]. While *Song et al.* did not observe large accelerated flows in their specific case, a multitude of reasons may account for this, e.g., the presence of reconnection at higher latitude [*Omidi et al.,* 1998]. In some circumstances, our magnetosheath-side discontinuity resembles an RD.

2. Simulation Model

The simulations are carried out with a 2-D hybrid code (kinetic ions; electrons: isothermal, massless fluid). The x-direction is across the magnetopause. The co-

[1]Also at Department of Electrical and Computer Engineering, University of California, San Diego, La Jolla

[2]Also at California Space Institute, UCSD.

Paper number 1999GL900211.
0094-8276/99/1999GL900211$05.00

planar **B** is in the $\pm y$ direction. Boundaries are free inflow/outflow; a zero gradient is maintained in the first two moments of the particle distribution (see *Forbes and Priest* [1987] for MHD). There is no injection at $t = 0$; however, due to resistivity reconnection proceeds, and a semi steady-state inflow-outflow develops. All quantities are normalized with respect to the magnetosheath (subscript (0); magnetosphere: subscript (1)). The density ratio is $n_1/n_0 = 0.1$, the magnetic field ratio is $B_1/B_0 = 1.37$, the proton temperature ratio is $T_{p1}/T_{p0} = 3.0$. The upstream proton beta is $\beta_{p0} = 1.0$, for the electrons $T_{e0}/T_{p0} = 0.1$. Two cases are presented in detail: anti-parallel magnetic field (shear angle 180°), and a finite guide field (out-of-plane component, shear angle 160°). The cell size is one sheath proton inertial length c/ω_p with wavenumber resolution $ck/\omega_p \sim 3$, the time step is 0.025 ${\Omega_p}^{-1}$ (inverse proton cyclotron frequency). We use 150×300 cells with initially 60 particles/cell everywhere, and 12,000 time steps. Assuming 23 particles/cm^3 and ${\Omega_p}^{-1} = 0.375$ s, the simulation domain is $\sim 1.12 R_E \times 2.25 R_E$ run for ~2 min. real time. Resistivity follows the standard model and is set in the center of the simulation box with a maximum scale length $\ell_\eta = 2c/\omega_p$, falling off away from the center with the same scale. No curvature is introduced at the beginning of the simulation.

3. Results and Discussion

Reconnection proceeds and two asymmetric plasmoids develop which at $t \sim 200\,{\Omega_p}^{-1}$ leave the simulation box, when we evaluate the sheath–magnetosphere transition. We first discuss the results of the coplanar case. Fig. 1 shows the z-component of the vector potential, i.e., the field lines in the x,y-plane. The total magnetic field B and out-of-plane component B_z are depicted in Fig. 2 for the top (northern) half of the simulation. The total magnetic field shows two discontinuities, (I) and (II), that separate along y and reach a distance of $\sim 20\ c/\omega_{pi}$ at the boundary (flare angle 7.6°).

Fig. 3 shows the magnetic field components, the total magnetic field, the density n, the temperatures parallel ($T_\parallel$) and perpendicular ($T_\perp$) to **B** and the two flow velocities v_x, v_y normalized with the Alfvén velocity v_A.

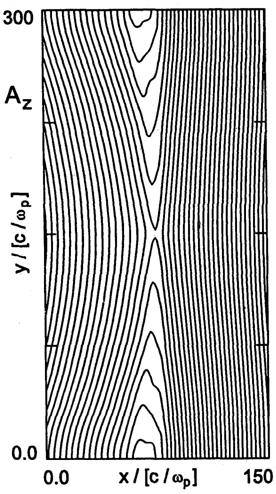

Figure 1. Magnetic field lines in x,y-plane (vector potential A_z) at time $t = 200\,{\Omega_p}^{-1}$, when plasmoids have left the simulation domain.

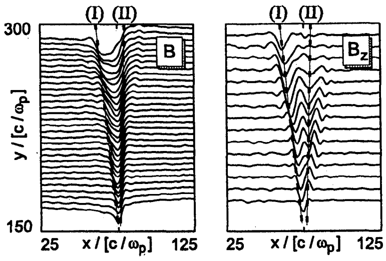

Figure 2. Stack plots of the total magnetic field B and the z component in the northern half of the simulation domain, with discontinuities (I) and (II), as indicated.

These cuts across the outflow are taken 125 c/ω_{pi} away from the x-line, averaged over 20 c/ω_{pi} in y. The course of B_x indicates that the same amount of reconnected flux corresponds to a larger x-distance in the sheath, leading to a larger curvature of the sheath field lines (Fig. 1). In Fig. 3, we have indicated the two discontinuities (dark shading) and their precursors (light shading). Between (I) and (II), which are about 4 to 8 c/ω_p wide, all plasma parameters are approximately constant. $B_y \sim 0$ indicates that both discontinuities are approximately of switch-off type. From resistive MHD, (I) is expected to be an IS. Here, we find that (I) does not match the anisotropic Rankine-Hugoniot (R-H) conditions [*Karimabadi,* 1995] of an IS near switch-off, primarily because a density jump is basically non-existent. Commonly, the density decreases slightly, whereas R-H predicts approximately 40% increase. The ion temperature jump is also less than predicted by 20% to 30%. While there is a small foot of backstreaming ions and an overshoot in $T_\parallel$, we do not find a significant temperature anisotropy far upstream or downstream that could account for this discrepancy. Note that the overshoot in $T_\parallel$, traditionally explained in terms of ions originating from the x-line, has a maximum at the discontinuity rather than at the separatrix, and thus is of local origin.

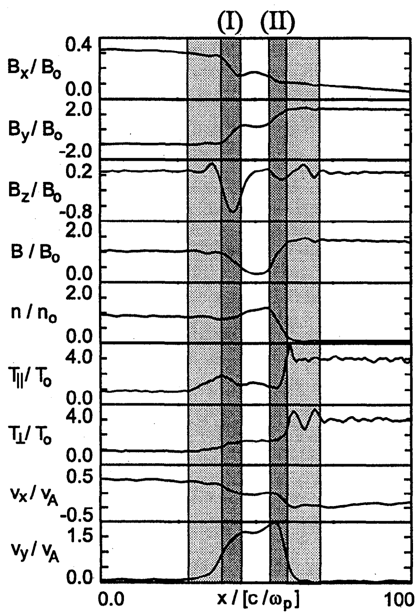

Figure 3. Magnetic field components, total field, density, parallel and perpendicular proton temperature, and x, y flow velocity 125 c/ω_{pi} from x-line. Dark shading: discontinuities (I), (II); light shading: precursors.

1-D simulations lack such accelerated ions and show a much larger foot of ions escaping from the downstream [*Krauss-Varban et al.*, 1995]. This is a strong indication that the 2-D geometry controls how (I) develops. Note that use of R-H conditions is only an approximation, and one may argue that higher order ion moments may play a role. However, given that R-H conditions are still reasonably well satisfied in 1-D simulations (which show more escaping ions), any such role must be minor. There is also an upstream wavetrain associated with (I).

At the magnetospheric side, there is a similar but narrower peak in $T_{\|}$. The upstream Alfvén wave does not form a standing wave train (Fig. 2), and there is a wave in the reverse direction. The jumps associated with (II) do not fit any conventional discontinuity. For the expected slow shock (SS), it has a reverse temperature jump. It cannot be a contact discontinuity (CD) because of a finite jump in B; moreover, a CD should disintegrate [*Omidi and Winske,* 1995]. There is no indication that this new type of kinetic discontinuity evolves over time. However, the 2-D geometry appears to be very important for its generation. We believe a detailed ion trajectory and thermalization study similar to *Lottermoser et al.* [1998] could be of benefit here.

Our results may appear similar to those of *Lin and Xie* [1997]. However, *Lin and Xie* interpret (I) as an IS. In addition, their significant density jump at (I) and temperature jump make (II) similar to a SS or a slow wave trailing an IS. The simulations by *Lin and Xie* have a large gradient of the upstream $|B|$ and n with distance from the x-line, and an anisotropy $T_{\perp} > T_{\|}$. As a consequence, their discontinuities change and conform more closely to MHD with distance from the x-line. In our simulations, there is just a weak (a few %) upstream, fast decompression in the vicinity of the x-line, and no significant gradient of the upstream quantities along y. Consequently, jumps (I) and (II) remain almost unchanged with distance from the x-line. We attribute the above differences to our boundary conditions, keeping the upstream ~ constant, which we believe is more representative of what occurs in nature.

For a finite guide field B_{z0} (shear angle 160°), the main differences to our results above are caused by the north-south asymmetry of the Hall current-generated B_z. In the lower (southern) portion of the simulation, the Hall generated field and pre-existing B_{z0} add in the transition layer. As a consequence, B does not develop as strong a minimum as for 180°. Also, energetic ions are almost absent and discontinuity (II) has no escaping rotational wave. Still, there are many similarities, such as the near switch-off character for (I) and (II).

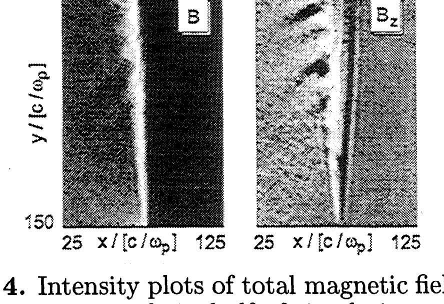

Figure 4. Intensity plots of total magnetic field B and z component in northern half of simulation, similar to Fig. 2, here for non-coplanar case (160°).

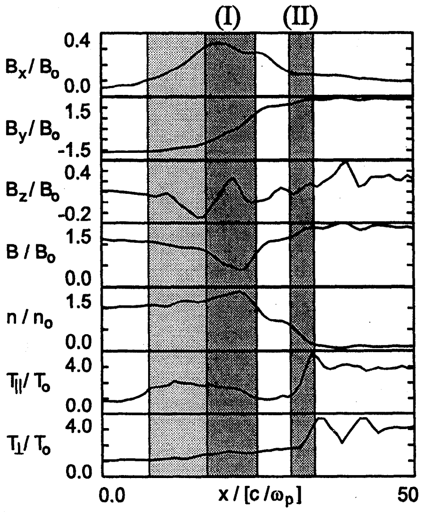

Figure 5. Same quantities as in Fig. 3, except for non-coplanar case (160° shear angle).

Consequently, (I) is neither an RD nor a TDIS, and the resistive MHD prediction that (I) is a TDIS except for a shear angle of 180° (TD), does not materialize.

In the northern part of the simulation, the two contributions to B_z subtract such that the total field reduces to ~0.2 B_o, while the ion β reaches ~15. At the same time, $T_{p\|}/T_{p\perp} \sim 1.3$ and ~2 a few c/ω_p upstream. As a consequence, the firehose instability criterion $\beta_{\|} - \beta_{\perp} - 2 > 0$ is satisfied, and the outflow and adjacent sheath become unstable. Fig. 4 shows B and B_z as an intensity plot. The instability has moderate amplitudes (~ 10% to 20% in B, n) but could clearly contribute to magnetosheath/magnetosphere mixing. The most important effect of the instability is on discontinuity (I): it now resembles more closely an RD, see Fig. 5 for a typical cut (the physical quantities now depend on y). Fluctuations caused by the firehose instability affect all field components. Also note that n and T_p are enhanced, whereas B is depressed within (I), which is consistent with 1-D simulations of left-handed (ion-sense) RDs [*Krauss-Varban et al.,* 1995] and indicates a similar current structure. Again, almost all of the jumps in n, T_p, and B occur at (II). We have made several runs at various shear angles (120°, 140°) and magnetospheric parameters, and find that the above results are typical. When the magnetospheric density is higher, discontinuity (I) resembles an RD more closely.

4. Summary

Conventional reconnection models are based on the assumption of 1-D discontinuities, and the upstream field line curvature changes from concave to convex behind the separatrix. Here we find that instead, the curvature remains concave downstream of the separatrix (Fig. 1). The shock normal angle θ_{Bn} changes from ~85° at 50 c/ω_p away from the center to ~80° at 120 c/ω_p, or 1.5° per convected ion gyroradius. While this has some effect on 1-D jump conditions, the mere fact that the plasma dependencies are 2-D is more important and opens up new solutions that are not accessible in 1-D. As a result, our 1-D cuts have no correspondence to known MHD solutions, even if anisotropy is taken into account. Comparison to 1-D simulations suggests that backstreaming ions are not a major factor.

Without a guide field B_{zo}, the discontinuities are of switch-off type, with almost no density change on the sheath side (I), and almost all of the density and temperature jump at the second discontinuity (II). There are three relevant propagating MHD discontinuities: SS, IS, and RD. It is sufficient to consider the scalar quantities B, n, and T. Since the anisotropy is small, an RD cannot account for the jumps in B or T by more than an order of magnitude. B_y suggests a solution close to switch-off, where the IS and SS merge. Close inspection shows a finite, but small rotation. Since the density jump at (I) is negative (~-10%) or non-existing but should be +40%, and in addition the temperature jump is off by 20 to 30%, (I) does not match R-H conditions. The situation is even more clear-cut for discontinuity (II), since both T and B decrease at the jump, unlike known discontinuities. Simulation cuts are very similar at different times and locations, and thus are not affected by noise. There is no indication of additional discontinuities as expected from MHD.

A finite guide field B_{zo} enters via its interaction with the Hall-generated [*Sonnerup,* 1979] field. The solution becomes asymmetric with respect to y: the south has a less pronounced B-minimum, and the north develops such a low B (high β), that an instability develops. For $B_{z0} < 0$, this asymmetry is reversed. Although the instability has moderate amplitudes, it causes the magnetosheath discontinuity to carry all of the field rotation, which makes it resemble an RD.

We have taken special care that our solutions are not influenced by restrictive boundary conditions. We do not find differences to runs that are 1/4 size, and our results concerning B, n, and T are very similar to simulations that include the curved bow shock and the Earth's dipole field, and as such do not depend on local boundary conditions [*Omidi et al.,* 1998]. But most convincingly, spacecraft observations simply do not show the succession of discontinuities predicted by MHD, and slow shocks are not generally observed at the magnetopause. Further, previous kinetic magnetopause reconnection simulations have not resulted in RDs, which are observed. In other observations, quite commonly, B is depressed in the transition region, with no significant change in n and only slight T enhancement with respect to the sheath [*Song et al.,* 1989; *C. T. Russell, J. Wygant* private communications]. Such observations are not only in good agreement with our results, but also necessitate a 2-D interpretation, since no 1-D jump conditions fit these observations. Finally, we like to add that the goal of this paper is not to explain a particular observation (which may have many interpretations), but rather to point out that reconnection solutions and associated discontinuities may be more complicated than previously appreciated.

Acknowledgments. The authors would like to thank K. B. Quest for helpful discussions. The work was supported by NASA's Space Physics Theory Program and NASW-97018, NSF grant ATM-9796051 at SciberNet, Inc., and NSF grant ATM-9614176 at UCSD. N. Omidi's work was performed under the auspices of the California Space Institute at UCSD. Computations were executed on Intel-based workstations at SciberNet, Inc. and on the Cray T-90 of the NSF San Diego Supercomputer Center.

References

Berchem, J., and C. T. Russell, Magnetic field rotation through the magnetopause: ISEE 1 and 2 observations, *J. Geophys. Res., 87,* 8139–8148, 1982.

Forbes, T. G., and E. R. Priest, A comparison of analytical and numerical models for steadily driven magnetic reconnection, *Rev. Geophys., 25,* 1583–1607, 1987.

Gosling, J. T., M. F. Thomsen, S. J. Bame, T. G. Onsager, and C. T. Russell, The electron edge of the low latitude boundary layer during accelerated flow events, *Geophys. Res. Lett.,, 17,* 1833, 1990.

Karimabadi, H., Physics of intermediate shocks: A review, *Adv. Space Res., 15,* 507–520, 1995.

Krauss-Varban, D. and N. Omidi, Large-scale hybrid simulations of the magnetotail during reconnection, *Geophys. Res. Lett.,, 22,* 3271–3274, 1995.

Krauss-Varban, D., H. Karimabadi, and N. Omidi, Kinetic structure of rotational discontinuities: Implications for the magnetopause, *J. Geophys. Res., 100,* 11,981-11,999, 1995.

Kuznetsova, M. M., M. Hesse and D. Winske, Ion dynamics in a hybrid simulation of magnetotail reconnection, *J. Geophys. Res., 101,* 27,351–27,373, 1996.

Levy, R.H., H.E. Petschek, and G.L. Siscoe, Aerodynamic aspects of the magnetospheric flow, *AIAA J., 2,* 2065, 1964.

Lin, Y., and L. C. Lee, Structure and reconnection layers in the magnetopause, *Space Sci. Rev., 65,* 59, 1993.

Lin, Y., and D. W. Swift, A two-dimensional hybrid simulation of the magnetotail reconnection layer, *J. Geophys. Res., 100,* 19,859–19,870, 1996.

Lin, Y., and H. Xie, Formation of reconnection layer at the dayside magnetopause, *Geophys. Res. Lett., 24,* 3145–3148, 1997.

Lottermoser, R.-F., M. Scholer, and A. P. Matthews, Ion-kinetic effects in magnetic reconnection: Hybrid simulations, *J. Geophys. Res., 103,* 4547–4559, 1998.

Omidi, N., and D. Winske, Structure of the magnetopause inferred from 1-D hybrid simulations, *J. Geophys. Res., 100,* 11,935–11,955, 1995.

Omidi, N., H. Karimabadi, and D. Krauss-Varban, Hybrid simulation of the curved dayside magnetopause during southward IMF, *Geophys. Res. Let., 25,* 3273-3276, 1998.

Petschek, H. E., Magnetic annihilation, in *AAS-NASA Symposium on the physics of solar flares,* edited by W. N. Hess, p. 425, 1964.

Russell, C. T., and R. C. Elphic, Initial ISEE magnetometer results: Magnetopause observation, *Space Sci. Rev., 22,* 681, 1978.

Scholer, M., Asymmetric time-dependent and stationary magnetic reconnection at the dayside magnetopause, *J. Geophys. Res., 94,* 15,099–15,111, 1989.

Song, P., C.T. Russell, N. Lin, R.J. Strangeway, J.T. Gosling, M. Thomson, T. A. Fritz, D. G. Mitchell, and R. R. Anderson, Wave and Particle Properties of the subsolar magnetopause, *Phys. of Space Plasmas, 89,* 463, T. Chang et al., eds., Scientific Publishers, Inc., Cambridge, MA, 1989.

Sonnerup, B. U. Ö., Magnetic field reconnection, *in: Solar System Plasma Physics,* Volume III, L. T. Lanzerotti et al., eds., North Holland Publ. Comp., 1979.

D. Krauss-Varban, H. Karimabadi and N. Omidi, SciberNet,Inc., 5414 Oberlin Drive, Suite 251, San Diego, CA, 92121. (e-mail: varban@scibernet.com)

(Received September 28, 1998; revised January 25, 1999; accepted February 17, 1999.)